

Photo-structuring of As₂S₃ glass by femtosecond irradiation

Saulius Juodkazis, Toshiaki Kondo, Hiroaki Misawa

*CREST-JST & Research Institute for Electronic Science, Hokkaido University, N21-W10,
Kita-ku, Sapporo 001-0021, Japan*

Saulius@es.hokudai.ac.jp; Misawa@es.hokudai.ac.jp

Andrei Rode, Marek Samoc, Barry Luther-Davies

*Laser Physics Centre, Research School of Physical Sciences and Engineering, the Australian
National University, Canberra ACT 0200, Australia*

Abstract: The nonlinear absorption coefficient of As₂S₃ glass has been measured to be 2.0 cm/GW for femtosecond pulses at 800 nm. Femtosecond laser structuring via two photon absorption in bulk As₂S₃ glass by erasable and permanent photo-darkening is demonstrated using both holographic and direct multi-beam laser writing.

© 2006 Optical Society of America

OCIS codes: (160.4330) Nonlinear optical materials; (210.4770) Optical recording; (350.3950) Micro-optics; (350.3850) Materials processing; (350.2770) Materials processing; (160.2750) Glass and other amorphous materials;

References and links

1. A. Zoubir, M. Richardson, C. Rivero, A. Schulte, C. Lopez, K. Richardson, N. Hô, and R. Valée, "Direct femtosecond laser writing of waveguides in As₂S₃ thin films," *Opt. Lett.* **29**, 748 – 750 (2004).
2. J.-F. Viens, C. Meneghini, A. Villeneuve, T. Galstian, E. Knystautas, M. Duguay, K. Richardson, and T. Cardinal, "Fabrication and characterization of integrated optical waveguides in sulfide chalcogenide glasses," *IEEE J. Lightwave Technol.* **17**, 1184 – 1191 (1999).
3. A. Zakery, Y. Ruan, A. V. Rode, M. Samoc, and B. Luther-Davies, "Low loss waveguides in ultrafast laser deposited As₂S₃ chalcogenide films," *J. Opt. Soc. Am. B* **20**, 1844 - 1852 (2003).
4. A. V. Rode, A. Zakery, M. Samoc, R. B. Charters, E. G. Gamaly, and B. Luther-Davies, "Nonlinear as-s chalcogenide films for optical waveguide writing deposited by high-repetition-rate laser ablation," *Appl. Surf. Sci.* **197-198**, 481 – 485 (2002).
5. C. B. Schaffer, J. Garcia, and E. Mazur, "Bulk heating of transparent materials using a high-repetition rate femtosecond laser," *Appl. Phys. A* **76**, 351 – 354 (2003).
6. S. Juodkazis, A. V. Rode, E. G. Gamaly, S. Matsuo, and H. Misawa, "Recording and reading of three-dimensional optical memory in glasses," *Appl. Phys. B* **77**, 361–368 (2003).
7. T. Kondo, S. Matsuo, S. Juodkazis, and H. Misawa, "A novel femtosecond laser interference technique with diffractive beam splitter for fabrication of three-dimensional photonic crystals," *Appl. Phys. Lett.* **79**, 725–727 (2001).
8. T. Kondo, S. Matsuo, S. Juodkazis, V. Mizeikis, and H. Misawa, "Three-dimensional recording by femtosecond pulses in polymer materials," *J. Photopolym. Sci. Technol.* **16**, 427–432 (2003).
9. B. K. Rhee, J. S. Byun, and E. W. VanStryland, "Z scan using circularly symmetric beams," *J. Opt. Soc. Am. B* **13**, 2720 – 2723 (1996).
10. M. Sheikh-Bahae, A. A. Said, T. Wei, D. J. Hagan, and E. W. Van Stryland, "Sensitive measurement of optical nonlinearities using a single beam," *IEEE J. Quantum Electron.* **26**, 760–769 (1990).
11. S. Matsuo, S. Juodkazis, and H. Misawa, "Femtosecond laser microfabrication of periodic structures using a microlens array," *Appl. Phys. A* **80**, 683 – 685 (2004).

Chalcogenide glasses are nonlinear optical materials with considerable potential for all-optical switching at the IR telecommunications wavelengths [1, 2, 3, 4]. A general characteristic of

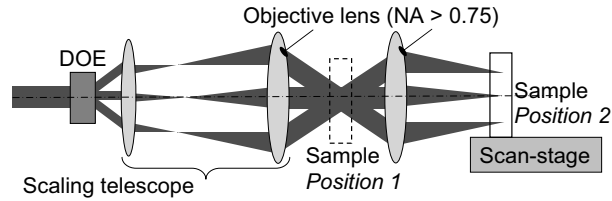


Fig. 1. Schematic setup based on diffractive optical element (DOE) for holographic (with sample position (1)) and direct multi-beam recording (sample position (2)), respectively.

chalcogenides is their susceptibility to photo-darkening which can result in a refractive index change of $\Delta n \sim 10^{-2}$ that can be used for creating thermally re-writable optical memories and for applications in micro-photonics.

This work explores the use of nonlinear absorption of femtosecond laser pulses to achieve permanent/erasable 3D optical data storage [5, 6] in a photosensitive chalcogenide glass - a process which has the potential to significantly boost memory storage capacity. Ultrafast (sub-1 ps) 800-nm laser pulses were focused into a block of transparent As_2S_3 glass to record a three-dimensional (3D) pattern via photo-darkening. The formation of "memory bits" involves two-photon absorption and can be achieved using relatively low energy laser pulses. This provides the opportunity for fast parallel writing of multi-bit patterns using a single laser pulse.

Commercial As_2S_3 glass (Amorphous Materials) with a melting temperature of 310°C was used in this study. Amplified femtosecond laser pulses (wavelength 800 nm, pulse duration 150 fs) were obtained from a Spectra Physics Hurricane laser operating at 1 kHz repetition rate. Holographic recording was realized by 4 and 5-beam interference using a diffractive optical element (DOE) (see, ref. [7, 8] for details) and focusing with a $NA = 0.75$ objective lens. For direct laser writing, the holographic setup was modified by simply adding a second lens (Fig. 1). In this geometry a DOE generating 31 beamlets (G1022A) in a single line was utilized and the sample was translated normal to the line thereby recording 31 lines in one scan. The scan speed was 0.1 mm/s speed which corresponded to 20 nm between successive pulses. The whole sample was then translated laterally by half the pattern width and re-exposed. By this process the line exposed to the most off-center beamlet (the weakest) was subsequently overwritten with the strongest 0th beamlet during the second scan resulting in the formation of a uniform pattern over a comparatively large ($\sim\text{cm}^2$) area.

The nonlinear absorption of As_2S_3 was measured between 650 nm and 1200 nm using the z-scan technique with a TOPAS (Light Conversion) optical parametric generator pumped with a femtosecond Clark-MXR CPA2001 laser. The beam from the TOPAZ was focussed into a sample 2.74 mm thick using an $f = 150$ mm lens and in some conditions spatially filtered with a pair of apertures to give a truncated Airy disk pattern as described in ref. [9]. Prior to running Z-scans on As_2S_3 the light intensity was calibrated using closed aperture Z-scans on fused silica plates 1-3 mm thick for which the nonlinearity is known to be $n_2 = 3 \times 10^{-16} \text{ cm}^2/\text{W}$.

Figure 2 shows a set of Z-scans recorded at 820 nm for a range of peak intensities. The curves were fitted by numerical integration of Sheikh-Bahae equations [10] to determine the nonlinear absorption parameters. As an example, Fig. 2(b) shows the fit for the lowest intensity from Fig. 2(a) ($0.839 \text{ GW}/\text{cm}^2$) which resulted in the imaginary part of the nonlinear phase shift $Im(\Delta\phi) = 0.30$ rad. A large number of data points were recorded at various intensities and from these it was determined that $Im(\Delta\phi)/I = 0.547 \text{ rad cm}^2/\text{GW}$ at 820 nm. Taking into account the sample thickness one calculates from $Im(n_2) = \frac{\lambda}{2\pi L} \frac{Im(\Delta\phi)}{I}$ that $Im(n_2) = 3.1 \times 10^{-14} \text{ cm}^2/\text{W}$ and, from $\beta = \frac{2\pi \cdot Im(n_2)}{\lambda}$ the two-photon absorption coefficient of $\beta = 2.0 \pm 0.2 \text{ cm}/\text{GW}$. Since

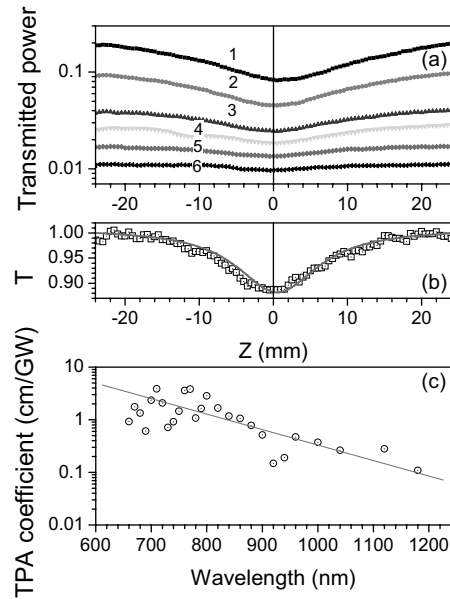


Fig. 2. Z-scan measurements. (a) A set of open aperture Z-scans at 820 nm for the following light intensities: 14.5, 7.2, 3.0, 2.1, 1.22 and 0.839 GW/cm². (b) Numerical fit of transmission, T , for the intensity of 0.839 GW/cm². (c) Wavelength dependence of the two-photon absorption coefficient; line is an exponential fit given as an eyeguide.

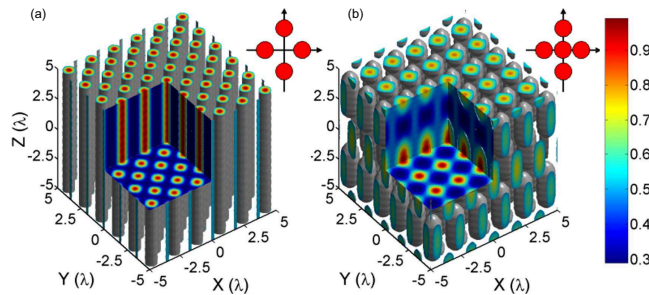


Fig. 3. Calculated normalized light intensity distribution of 4 (a) and 5 (b) beams (assumed to be plane waves) hologram. The angle between side beams and optical axis was $\theta = 33.8^\circ$; the ratio of E-fields of interfering beams was (1 : 1 : 1 : 1) and (1 : 1 : 1 : 1 : 4(*central*)) for 4 and 5-beams, respectively. The lateral pattern (xy -cross-section) of recording beams is shown as insets. The lateral periods are given by $d = \sqrt{2}\lambda / (2\sin\theta)$ (4-beams) $d = \lambda / \sin\theta$ (5-beams) and the axial $d = \lambda / (1 - \cos\theta)$ (5-beams), where θ the angle between the side beam and optical axis.

the two-photon absorption cross section can be expressed as $\sigma_2 = \frac{\beta\hbar\omega}{N}$ and the molecular density of As₂S₃ molecules is $N = N_0 \frac{\rho}{M} \simeq 7.8 \times 10^{21} \text{ cm}^{-3}$, we obtain $\sigma_2 = 6.2 \times 10^{-50} \text{ cm}^4\text{s}$ or 6.2 Goepfert-Mayers (GM) for a formally stoichiometric molecule.

The wavelength dependence of the two-photon absorption coefficient for As₂S₃ obtained from Z-scans at different wavelengths is shown in Fig. 2. The scatter in the results primarily arises from uncertainties in determining the intensity in the samples and the possibility that at high intensity the approximation used in the Sheikh-Bahae theory [10] was broken and higher-

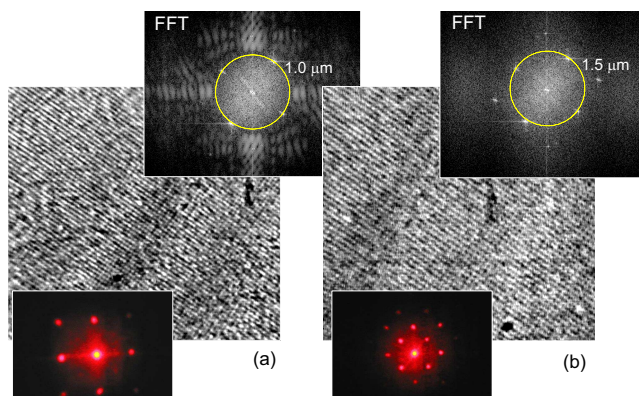


Fig. 4. Optical transmission images of four (a) and five (b) beams holograms and their Fourier transform images: numerical (upper inset) and by diffraction readout by 632 nm laser light (lower inset). Theoretical period was $1.02 \mu\text{m}$ (4-beams) and $1.45 \mu\text{m}$ (5-beams). Holograms were recorded by a 5 min exposure to the $3 \mu\text{J}/\text{pulse}$ (at 1 kHz repetition rate) pulses of 800 nm wavelength and 150 fs duration. Area of pattern 0.7 mm at $20 \mu\text{m}$ depth; angle of focusing was 33.6° .

order absorption could affect the measurements. The large amount of data collected at 820 nm - close to the wavelength used in the experiments on two-photon induced photo-darkening - led to better accuracy at this wavelength.

The laser intensity thresholds for erasable and permanent two-photon photo-modification were measured and compared with those for conventional single-photon direct laser writing using a cw-laser [2, 3, 4]. The single pulse threshold for erasable photo-darkening for a 800 nm/180 fs pulse was determined by focused beam direct laser writing to be $5.7 \pm 0.5 \text{ GW}/\text{cm}^2$ ($\sim 1 \text{ mJ}/\text{cm}^2$) for three-dimensional patterns written approximately $20 \mu\text{m}$ beneath the surface using the $NA = 0.75$ objective lens. Erasing was achieved by annealing the sample at $150 \pm 15^\circ\text{C}$ for 2 h. The threshold was determined using a beam with minimised spherical aberration by changing the divergence of incoming beam to achieve photodarkening with the smallest cross-section at the smallest pulse energy at a fixed $20 \mu\text{m}$ depth beneath the target surface. Near the threshold irradiance lines of exposures using single pulse separated by 400 nm were created and this allowed the onset of photo-modification to be clearly identified by *in situ* observation. The dielectric breakdown threshold recognizable by a plasma spark occurred at approximately $\sim 0.18 \text{ J}/\text{cm}^2/\text{pulse}$ ($8.2 \times 10^{11} \text{ W}/\text{cm}^2/\text{pulse}$ irradiance). Such fluences are obtainable from standard fs-oscillator [5], however, we used an amplified laser at 1 kHz repetition rate and lower average power to avoid the heat accumulation present in a experiments with MHz oscillators. The single pulse threshold fluence at 1 kHz was significantly ($> 10^2$ times) smaller than that observed in experiments with fs-/MHz-lasers [1] but the irradiance was larger. Permanent (thermally un-erasable) photodarkening was observed at approximately $10^{-2} \text{ J}/\text{cm}^2$ using the same measurement procedure.

It should be noted that the data on photodarkening discussed in what follows were strongly affected by spherical aberration and also involved multiple pulses, hence, the thresholds determined above can not be directly compared with fluence/irradiance used in the following experiments.

Four and five beams holograms were formed inside As_2S_3 glass to check a possibility of recording a 3D hologram by photodarkening. The light intensity distribution $I(\mathbf{r})$ creating the

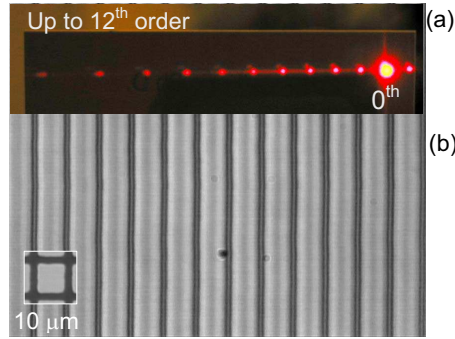


Fig. 5. (a) Diffraction pattern of HeNe laser beam on the grating recorded by direct multi-beam (with 31 inline beams) laser writing. (b) Optical image of the grating in As_2S_3 glass.

hologram can be simulated by interference of plane waves as:

$$I(\mathbf{r}) = \sum_{n,m} \mathbf{E}_n e^{-i(\mathbf{k}_n \cdot \mathbf{r} + \delta_n)} \cdot \mathbf{E}_m^* e^{i(\mathbf{k}_m \cdot \mathbf{r} + \delta_m)}, \quad (1)$$

where \mathbf{E} is the E-field vector (* designates a complex conjugate), \mathbf{r} is the coordinate vector, \mathbf{k} the wavevector, and $n = m$ represents the number of interfering beams. The phases of beams are given by $\delta_{n,m} = 0$. Control of the phases provides a method for fine tuning of the interference patterns. Calculations were carried out for s-polarization (perpendicular to the plane of incidence), hence there was no depolarization present, i.e., the longitudinal component $E_z = 0$ (Fig. 3).

The resulting optical images of the pattern of photodarkening formed holographically are shown in Fig. 4. These images were digitised and Fourier transformed numerically. The resulting calculated diffraction patterns are shown in the inset with the dominant (smallest) period identified and this corresponded well to the theoretically determined value appropriate for the focusing conditions employed in the experiment. The diffraction pattern of He-Ne beam (see lower inset) was also recorded and shows the same periodicity. This implies, however, that the actual pattern recorded by 4-/5-beams inside glass was planar rather than three-dimensional as expected, i.e. the optical diffraction was the same as calculated from 2D optical transmission image.

The actual axial length of the 4-/5-beams pattern was evaluated by measuring the angular dependence of the diffraction efficiency from a grating recorded by two beam interference. The first minimum of the diffraction was observed at 29° at largest saturated value of photodarkening. The highest photodarkening value of $\Delta n = 0.06$ (at 633 nm) was obtained in As_2S_3 [3, 4]. Then, the 29° corresponds to $10 \mu\text{m}$ axial length. At the third of the saturated exposure, $\Delta n = 0.02 \pm 0.005$, the position of the first minimum of the angular dependence of diffraction efficiency was 18° , which corresponds to the axial extent (thickness) of a photodarkened region $d = 20 \pm 5 \mu\text{m}$. It is noteworthy, that in order to avoid total internal reflection and to measure the transmitted first-order diffraction, the cover glass was attached onto the back side of As_2S_3 sample using immersion oil ($n = 1.515$ at 633 nm). This expanded the angular range of the measurable diffraction up to 30° .

The depth of the pattern formed by 4-/5-beams inside the As_2S_3 Sample was considerably smaller than would be expected from the focusing conditions. The effective numerical aperture of beams writing the pattern was 5-6 times smaller than that of the objective lens, $NA = 0.75$, since the diameter of the beamlets was approximately 1 mm (the entrance aperture of the objective lens was 5 mm). Hence, the axial extent of the waist (the depth of focus), was expected to be

approximately $50\ \mu\text{m}$. The experimentally measured axial extent of the photodarkened region of only $d = 20 \pm 5\ \mu\text{m}$, was also confirmed by direct optical imaging. The discrepancy between the theoretical and experimental length of the pattern can be explained by the photodarkening itself, which creates an array of micro-lenses which modify the distribution of the light preventing hologram formation deeper into the sample. This is a fundamental constraint of 3D structuring: once the refractive index is changed, the focusing is altered for the regions further along the light propagation. In the case of holographic recording, the 3D intensity distribution (Fig. 3) was distorted when photo-darkening occurred at locations of the highest intensity. The 3D structures still could be recorded by translating sample axially in steps equal to the axial period along the direction of light propagation.

The simple addition of one lens allowed us to change the holographic recording setup into a multi-beam direct laser writing tool (the sample position 2 in Fig. 1). Such extension of the holographic recording is equivalent to the more efficient photo-structuring by a lens array introduced recently [11]. The effective numerical aperture of the objective lens for multi-beam recording becomes smaller by the ratio of the beamlet diameter to that of entrance aperture of the objective lens. The pattern of lines written by slow scanning using the lateral shift described earlier has proved to create extended gratings with high structural quality. The pattern could not be erased by a $150^\circ\text{C}/2\ \text{h}$ annealing procedure (no changes of optical density were observed). This method can be used for waveguide formation as well.

Rewritable and permanent photo-structuring of As_2S_3 glass by femtosecond laser pulses has been demonstrated. Both methods can be applied for efficient large-area ($\sim\text{mm}$) pattern formation. The two-photon absorption coefficient was measured for As_2S_3 chalcogenide glass in a wide spectral range from 650 to 1200 nm. The two-photon absorption cross-section was found to be $6.2 \pm 0.5\ \text{GM}$ around 800 nm wavelength. The threshold laser intensities for erasable and permanent photodarkening for single 800 nm/180 fs pulses were $1\ \text{mJ}/\text{cm}^2/\text{pulse}$ and $10\ \text{mJ}/\text{cm}^2/\text{pulse}$ (dielectric breakdown at $\sim 0.18\ \text{J}/\text{cm}^2/\text{pulse}$) correspondingly in As_2S_3 . The results demonstrate that the use of chalcogenide media modified by ultrafast laser pulses through a photodarkening process has a great potential for fast 3D laser writing of erasable and permanent memory approaching a TBits/cm^3 memory density domain (estimated from a single bit volume $\lambda \times \lambda \times 2\lambda$ at focusing with objective lens of $NA = 0.75$).

The support of the Australian Research Council through its Federation Fellow and Discovery programs is gratefully acknowledged.